Inorganic Chemistry Communications 13 (2010) 613–617

Contents lists available at ScienceDirect

Inorganic Chemistry Communications

journal homepage: www.elsevier.com/locate/inoche

Synthesis, crystal structure and photophysical properties of a novel Pt(II) complex with multi-functionalized cyclometalating ligand

Dongfang Qiu [a,*], Yuquan Feng [a], Hongwei Wang [a], Xiaoyu Bao [a], Yingchen Guo [a], Yanxiang Cheng [b], Lixiang Wang [b]

[a] College of Chemistry and Pharmacy Engineering, Nan yang Normal University, Nan yang, 473061, PR China
[b] State Key Laboratory of Polymer Physics and Chemistry, Changchun Institute of Applied Chemistry, Chinese Academy of Sciences, Changchun, 130022, PR China

ARTICLE INFO

Article history:
Received 3 February 2010
Accepted 23 February 2010
Available online 1 March 2010

Keywords:
Platinum (II)
Cyclometalated
Multi-functionalized
Crystal structure
Photophysics

ABSTRACT

A novel Pt(II) complex [(L)PtCl] (HL = 4-{*p*-[N-(4-(9-carbazole))butyl-N-phenyl] aniline}-6-phenyl-2,2′-bipyridine) has been synthesized and verified by ^{1}H NMR, elemental analysis and X-ray crystallography. The crystal ($C_{44}H_{35}N_4ClPt$, $M_r = 850.30$) belongs to monoclinic system, space group $P2(1)/c$, with $a = 21.864(6)$, $b = 9.306(3)$, $c = 17.240(5)$ Å, $\beta = 96.483(6)°$, $Z = 4$, $V = 3485.3(16)$ Å^3, $D_C = 1.620$ g/cm^3, μ(Mo-Kα) = 4.141 mm^{-1}, $F(000) = 1688$, $R_1 = 0.0591$, $wR_2 = 0.0976$. The coordinate geometry of the Pt atom is a distorted square planar configuration. The complex molecules are stacked by a weak π–π interaction in a head-to-tail fashion along the *b* axis to form 1D chain and the alternating 1D chains are packed to form the 2D lamellar system. The complex shows an intense metal-to-ligand charge transfer (^{1}MLCT) ($d\pi(Pt) \rightarrow \pi^*(L)$) transitions ($\varepsilon \sim 2 \times 10^4$ dm^3 mol^{-1} cm^{-1}) at 448 nm in the UV–Vis absorption spectrum and a strong phosphorescence at 592 nm in CH_2Cl_2 solution at room temperature. An intramolecular energy transfer process from the carbazole unit to the arylamine-modified [(C^N^N)PtCl] emissive center exists in the complex.

Cyclometalated Pt(II) complexes with the (C^N^N) tridentate ligand have recently received considerable interest in organic light-emitting diodes (OLEDs) [1–5]. At room temperature, [(C^N^N)Pt] complexes are phosphorescent emitting materials with high quantum yields since the strong ligand field effect of the cyclometalated carbon raises the energy of the *d*–*d* transitions, the moderate σ-donating and π-accepting abilities of (C^N^N) ligand properly satisfy the demand of the Pt(II) coordination geometry of the square plane to discourage the D_{2d} distortion which is likely to result in a non-radiactive decay [6,7].

Our group [8] integrated hole-transporting arylamine into the [(C^N^N)Pt] phosphorescent emitting center to form a novel class of multifunctional complexes. The bathochromically shifted maxima in the absorption and emission spectra indicate that the incorporation of an electron-rich group into the electron-deficient pyridine moiety can strengthen the donor–acceptor (D–A) interaction. The resulting complexes display stronger phosphorescence in CH_2Cl_2 solutions at room temperature with relatively higher quantum yields and much longer lifetimes. An orange multilayer organic light-emitting diode, used [(L^2)PtCl] (HL^2 = 4-[*p*-(N-butyl-N-phenyl)anilino]-6-phenyl-2,2′-bipyridine) as phosphorescent dopant, was fabricated, achieving a maximum current efficiency of 11.3 cd A^{-1} and a maximum external efficiency of 5.7%.

Carbazole and its derivatives are classic blue-emission and electro-active materials, widely utilized as hosters and charge transporters in OLEDs [9–11], conductive electropolymers [12,13], and electrochromic polymers [14]. In this paper, we further introduced a carbazole unit into [(L^2)PtCl] complex through alkyl chain to form tri-functional complex and studied its photo-physical behaviors. The fundamental design considerations are to 1) integrate the hoster and dopant into one molecule to simplify the production process of OLEDs; 2) maintain spectral property of each component separately, which can help to study the interaction between them by selective optical- and electro-stimulation.

The synthesis of ligand and complex explored in this work are shown in Scheme 1. Carbazole directly coupled with excess 1, 4-dibromobutane under strong basic condition to afford 9-(4-bromobutane)carbazole (1) [15]. 4-(*p*-bromophenyl)-6-phenyl-2,2′-bipyridine was obtained using Kröhnke's method [16]. The powerful palladium-catalyzed Buchwald method and the efficient Pd(OAc)$_2$/DPEphos catalyst/ligand system [17] were adopted to facilitate the condensation of aniline with 4-(*p*-bromophenyl)-6-phenyl-2,2′-bipyridine. Then the resulting intermediate (**2**) reacted with 9-(4-bromobutane) carbazole (1) to afford the ligand HL (3) [18]. The cyclometalated Pt(II) chloride 4 was synthesized by refluxing the ligand HL (3) and K_2PtCl_4 in glacial acetic acid for 24 h in over 80% yield [19].

The single crystal of 4 was grown by slowly evaporating the solvent from its concentrated CH_2Cl_2/MeOH solution; its crystal data and crystal structure parameters are listed in Table 1 and the details of

---

* Corresponding author. Tel./fax: +86 377 63513595.
E-mail address: qiudf2008@gmail.com (D. Qiu).

1387-7003/$ – see front matter © 2010 Elsevier B.V. All rights reserved.
doi:10.1016/j.inoche.2010.02.016

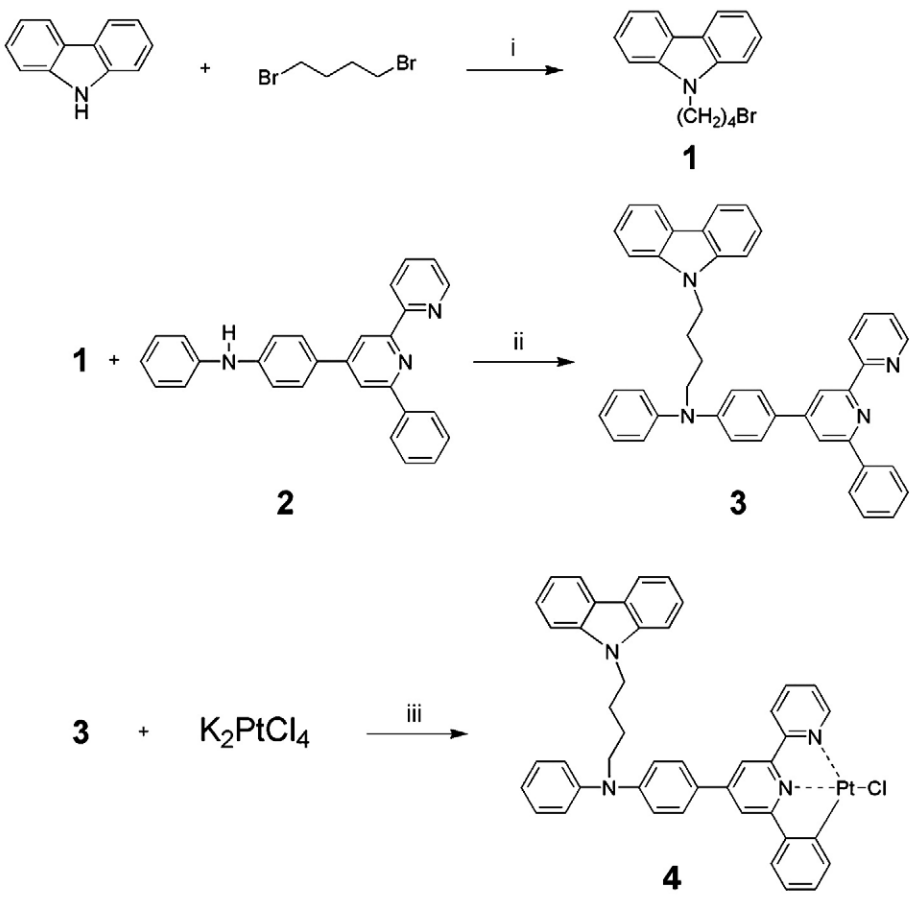

(i) $KOH/Bu_4NBr/THF/H_2O$, reflux 18h; (ii) NaH/THF, reflux overnight; (iii) HAc, reflux 24h.

Scheme 1. Synthetic route of the Pt(II) complex.

Table 1
Crystal data and crystal structure parameters.

Complex	Value
Empirical formula	$C_{44}H_{35}ClN_4Pt$
Formula weight	850.30
Temperature/K	296(2)
Wavelength/Å	0.71073
Crystal system	Monoclinic
Space group	*P*2(1)/*c*
a/Å	21.864(6)
b/Å	9.306(3)
c/Å	17.240(5)
α/(°)	90.00
β/(°)	96.483(6)
γ/(°)	90.00
Volume/$Å^3$	3485.3(16)
Z	4
D_c/(mg m^{-3})	1.620
Absorption coefficient/mm^{-1}	4.141
F(000)	1688
Crystal size/mm	$0.17 \times 0.14 \times 0.07$
θ range for data collection/(°)	2.38 to 25.00
Limiting indices	$-17 \leq h \leq 25, -11 \leq k \leq 10, -20 \leq l \leq 20$
Completeness to $\theta = 25.00°$	99.5%
Data/restraints/parameters	6101/2/451
Goodness-of-fit on F^2	0.931
Final *R* indices [$I > 2\sigma(I)$]	$R_1 = 0.0591$, $wR_2 = 0.0841$
R indices (all data)	$R_1 = 0.1566$, $wR_2 = 0.0976$
Largest diff. peak and hole/(e $Å^{-3}$)	1.180 and−0.978

the data collection, structure solution and refinement are given in [20]. Fig. 1 shows the perspective view of complex 4. The coordinate geometry of the Pt atom is a distorted square planar configuration with the C(1)-Pt(1)-N(2) and N(1)-Pt(1)-Cl(1) angles of 160.72(16) and 179.30(11)°. The bond distances of Pt-C(1), Pt-N(1) and Pt-N(2) are 2.021(4), 1.868 (3) and 2.082 (4) Å, respectively, which are comparable to those of previously reported analogous [21–24]. The configuration of C^N^N ligand is basically a plane with the C(1)-C(6)-C(7)-N(1) and N(2)-C(12)-C(11)-N(1) torsion angles of 2.40 and 0.76°. The dihedral angle between the phenyl ring at 4-position of the C^N^N ligand and the plane of the [(C^N^N)Pt] moiety is 23.75°. The geometry of the N(3) atom is a distorted tetrahedral configuration with the C(20)-N(3)-N(28), C(20)-N(3)-N(29) and C(28)-N(3)-N(29) angles of 119.3(4), 120.2(4) and 115.6(4)°. The peripheral carbazole unit is approximately a plane with the C(37)-C(38)-C(39)-C(40) torsion angle of 4.75°.

Instead of forming a continuous chain with Pt–Pt linkage in [(C^N^N)PtCl] [23,24] or a alternating arranged dimer [8], the complex molecules are stacked in a head-to-tail fashion along the *b* axis to form 1D chain (Fig. 2) with a Pt–Pt distance of 6.245 Å, suggesting no metal–metal interaction. The [(C^N^N)PtCl] moieties are almost parallel with the least dihedral angle of 0.106°, and their interplanar separation of 3.383 Å indicates that they are likely to be held together by a weak π–π interaction. The alternating 1D chains are packed to form the 2D lamellar system with the dihedral angle of 82.620° between the [(C^N^N)PtCl] moieties in neighboring chains.

Table 2 summarizes the absorption maxima and extinction coefficients of the absorption bands for the obtained compounds

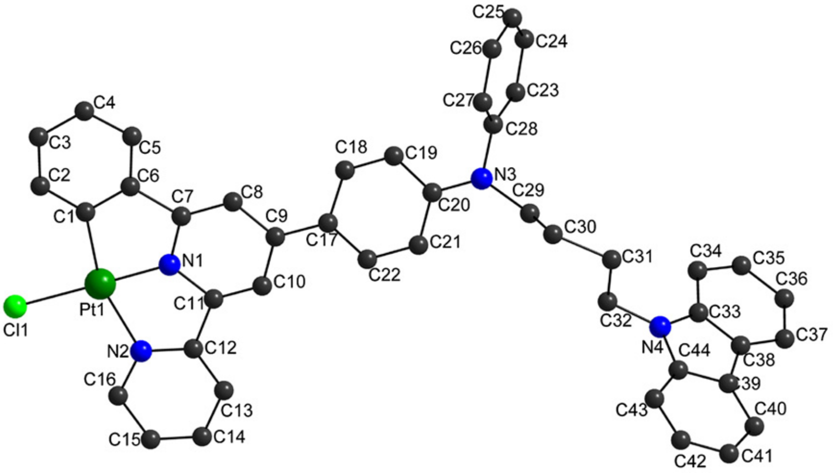

Fig. 1. Perspective view of 4 with the numbering scheme adopted (hydrogen atoms have been omitted for clarity).

and Fig. 3 shows the long-wavelength region of the absorption spectra for ligand HL (3) and the corresponding Pt (II) complex (4). The intense absorption bands in the high-energy region (λ<376 nm) with extinction coefficients (ε) of the order of 10^4 dm^3 mol^{-1} cm^{-1} were observed in the absorption spectra of 3 and 4, which are dominated by ^{1}IL ($\pi\rightarrow\pi^*$) transitions, while the low-energy band with λ_{max} at 448 nm in the absorption spectrum of 4 is assigned to the spin-allowed singlet $d\pi(Pt)\rightarrow\pi^*(L)$ metal-to-ligand charge transfer (^{1}MLCT) transitions. Owing to the strong D–A interaction between the amine unit and the C^N^N cyclometalating ligand [8], the molar extinction coefficient of the MLCT band is 2–3 times larger than those of the reported C^N^N cyclometalated Pt(II) complexes [1,2]. Compared to that of the reported complex [(L^2)PtCl], no apparent change in the long-wavelength region of the absorption spectrum was observed for 4, suggesting the introduction of carbazole unit through alkyl chain has no influence on the energy level of the [(L^2)PtCl] moiety.

The PL properties of compounds in CH_2Cl_2 solution are listed in Table 3. Three distinct emission bands are observed for 9-(4-Bromobutane)carbazole (**1**) in CH_2Cl_2 solution and in solid state

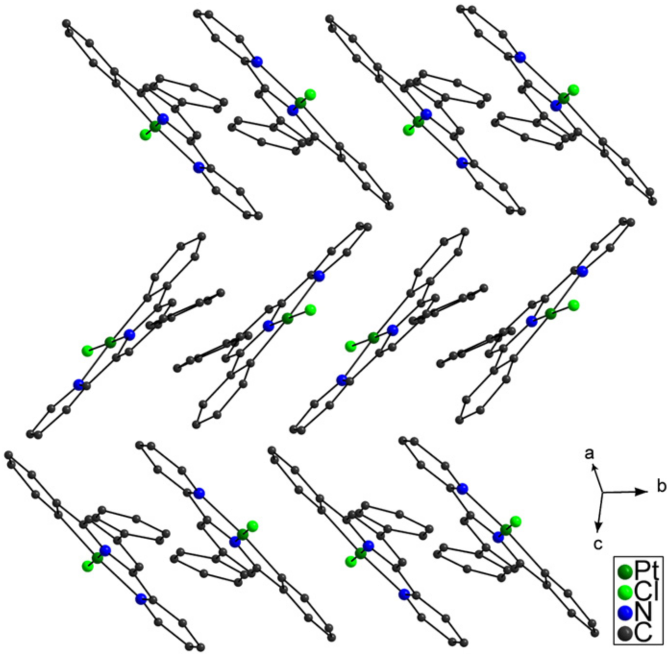

Fig. 2. 2D lamellar packing diagram of 4 (hydrogen atoms and the Carbazole-substituted phenylamino units have been omitted for clarity).

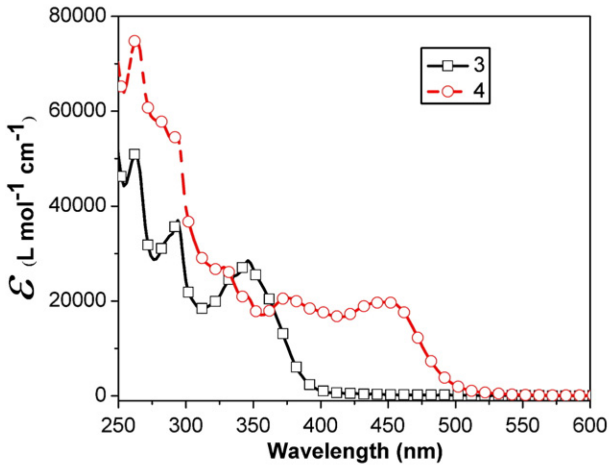

Fig. 3. UV–vis absorption spectra of ligand HL (3) and complex (4).

Table 2
Absorption maxima of the compounds in CH_2Cl_2 solutions at 298 K.

Compound	λ_{max}(nm)($\varepsilon\times10^3$ dm^3 mol^{-1} cm^{-1})
1	332(3.5), 294(14.0), 264(20.0)
3	346(28.5), 294(37.0), 262(50.9)
4	448(19.8), 376(20.6), 328(27.2), 294(55.3), 264(75.3)
[(L^2)PtCl]	449(20.6), 373(18.6), 327(21.4), 279(33.3)

Table 3
PL data of the compounds.

Compound	λ_{max}(nm)(Φ[a])	λ_{max}(nm)	λ_{max}(nm)
	In fluid solution[b]	In alcoholic glass[c]	In solid states (298 K)
1	350, 368, 385(sh)	–	418, 436, 460(sh)
3	462	–	446
4[d]	592(0.10)	582, 622	612
[(L^2)PtCl][d]	595(0.11)	581, 624	604, 625(sh)

[a] $[Ru(bpy)_3](PF_6)_2$ in degassed acetonitrile at 298 K ($\Phi_r=0.062$) as reference.
[b] Measured in degassed CH_2Cl_2 solutions at 298 K (concentration~1×10^{-5} mol dm^{-3}).
[c] Measured in $CH_3OH/C_2H_5OH=1/4$ (V/V) at 77 K.
[d] Excitation wavelength: 450 nm.

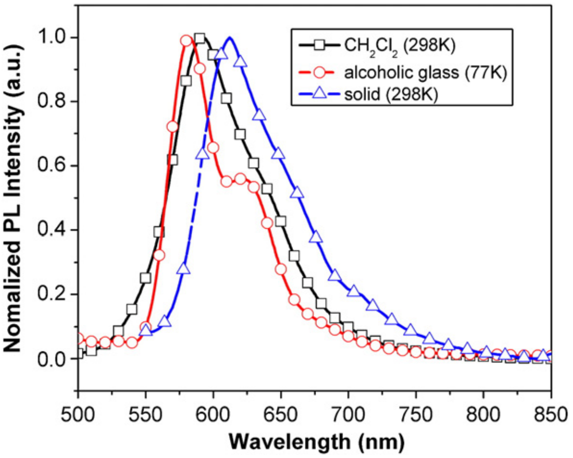

Fig. 4. Normalized PL spectra of 4 in dichloromethane solution at 298 K, in an alcoholic glass (4: 1 EtOH/MeOH) at 77 K and in solid state at 298 K.

respectively. Compared to the ones in CH$_2$Cl$_2$ solution, the large bathochromic shifts of three emission bands in solid state indicate the strong effect of molecular aggregation. Ligand HL (3) shows a blue emission band at 462 nm in CH$_2$Cl$_2$ solution, which is blue-shifted to 446 nm in solid state due to the steric hindrance effect.

For the multi-component complex 4, the selective optical-stimulation experiments were conducted. Excited at 450 nm, which was into the Pt(II)-based MLCT absorption band, complex 4 displays a strong emission at 592 nm with relatively high quantum yield of 0.10 in CH$_2$Cl$_2$ solution at 298 K, and it demonstrates PL maxima at 600, 594 and 590 nm in methanol, ethyl acetate and toluene solutions, respectively. While a negative solvatochromic effect is observed for its MLCT absorption wave ($\lambda_{\max}$ at 438, 438, 448 and 470 nm in methanol, ethyl acetate, CH$_2$Cl$_2$ and toluene solutions respectively), indicating the Stokes shift increases with strengthening solvent polarity. At 77 K in alcoholic glass, complex 4 shows well-resolved vibronic emission profile at 582 nm and 622 nm, respectively (Fig. 4). In solid state, a red-shifted emission band at 612 nm is observed arising from the π–π interactions between neighboring [(C^N^N)PtCl] moieties, which is in accordance with the result of the Crystal Structure section. The large Stokes shift, solvatochromic effect and temperature dependence suggest that the emission of complex 4 originates from the spin-forbidden triplet excited state. And its emission behaviors are almost as same as those of the reported complex [(L^2)PtCl] [8]. Excited at 320 nm, which was into the carbazole absorption band in the UV region, complex 4 displays two characteristic emission bands at ca. 350 and 592 nm, respectively. The higher energy carbazole-based emission band dramatically quenched, compared with those of 9-(4-Bromobutane)carbazole (1) and the physical mixture of 9-(4-Bromobutane) carbazole (1) and complex [(L^2)PtCl] (molar ratio = 1:1) under the same experimental condition. The quenching efficiency ($[1-(A/A_0)]\times 100(\%)$) is 85.8%, in which A and A_0 stand for the integrated area from 320 nm to 500 nm in the emission spectra of complex 4 and 9-(4-Bromobutane)carbazole (1), respectively. While the intensity of the latter band clearly increased compared to that of complex [(L^2)PtCl]. These results suggest that an intramolecular energy transfer process from the carbazole unit to the arylamine-modified [(C^N^N)PtCl] emissive center exists in complex 4. The studies on OLEDs and electrochemistry are in progress and will be reported in another paper.

Acknowledgments

This work is supported by the National Natural Science Foundation of China (No. 50673088), Science Fund for Creative Research Groups (No. 20621401) and 973 Project (2009CB623600).

Appendix A. Supplementary material

Supplementary data associated with this article can be found, in the online version, at doi:10.1016/j.inoche.2010.02.016.

References

[1] W. Lu, B.-X. Mi, M.C.W. Chan, Z. Hui, N. Zhu, S.T. Lee, C.-M. Che, Chem. Commun. (2002) 206–207.

[2] W. Lu, B.-X. Mi, M.C.W. Chan, Z. Hui, C.-M. Che, N. Zhu, S.-T. Lee, J. Am. Chem. Soc. 126 (2004) 4958–4971.

[3] S.C.F. Kui, I.H.T. Sham, C.C.C. Cheung, C.-W. Ma, B. Yan, N. Zhu, C.-M. Che, W.-F. Fu, Chem. Eur. J. 13 (2007) 417–435.

[4] B.-P. Yan, C.C.C. Cheung, S.C.F. Kui, V.A.L. Roy, C.-M. Che, S.-J. Xu, Appl. Phys. Lett. 91 (2007) 063508.

[5] B.-P. Yan, C.C.C. Cheung, S.C.F. Kui, H.-F. Xiang, V.A.L. Roy, S.-J. Xu, C.-M. Che, Adv. Mater. 19 (2007) 3599–3603.

[6] S.-W. Lai, M.C.-W. Chan, T.-C. Cheung, S.-M. Peng, C.-M. Che, Inorg. Chem. 38 (1999) 4046–4055.

[7] W. Lu, M.C.W. Chan, N. Zhu, C.-M. Che, C. Li, Z. Hui, J. Am. Chem. Soc. 126 (2004) 7639–7651.

[8] D.F. Qiu, J. Wu, Z.Y. Xie, Y.X. Cheng, L.X.J. Wang, Organomet. Chem. 694 (2009) 737–746.

[9] J.Q. Ding, B. Wang, Z.Y. Yue, B. Yao, Z.Y. Xie, Y.X. Cheng, L.X. Wang, X.B. Jing, F.S. Wang, Angew. Chem. Int. Ed. 48 (2009) 6664–6666.

[10] Q. Wang, J.Q. Ding, D.G. Ma, Y.X. Cheng, L.X. Wang, F.S. Wang, Adv. Mater. 21 (2009) 2397–2401.

[11] J.Q. Ding, J.H. Lu, Y.X. Cheng, Z.Y. Xie, L.X. Wang, X.B. Jing, F.S. Wang, Adv. Funct. Mater. 18 (2008) 2754–2762.

[12] R. Clergereaux, I. Séguy, P. Jolinat, J. Farenc, P. Destruel, J. Phys. D: Appl. Phys. 33 (2000) 1947–1952.

[13] G. Inzelt, J. Solid State Electrochem. 7 (2003) 503–510.

[14] J. Natera, L. Otero, L. Sereno, F. Fungo, N.-S. Wang, Y.-M. Tsai, T.-Y. Hwu, K.-T. Wong, Macromolecules 40 (2007) 4456–4463.

[15] Synthesis of 9-(4-Bromobutane)carbazole (1): To a mixture of KOH (11.2 g) and nBu4NBr in H$_2$O (20 mL) was added dropwise a solution of carbazole (6.68 g, 40.0 mmol) and 1, 4-dibromobutane (20 mL, 160 mmol) in THF (80 mL), and the mixture was refluxed for 18 h. After the mixture was cooled to room temperature, the product was extracted with dichloromethane, washed with distilled water, and dried over anhydrous sodium sulfate and concentrated. The product mixture was purified by column chromatography (silica gel, petroleum ether : CH$_2$Cl$_2$ = 2: 1 (V/V)). 9-(4-bromobutane)carbazole was obtained as white needle crystal by recrystallizing from MeOH/Ethyl Acetate solution: 9.5 g (yield: 78.5%). 1H NMR (300 MHz, CDCl$_3$): δ 8.10 (d, J = 7.8 Hz, 2H), 7.49–7.38 (m, 4H), 7.26–7.12 (m, 2H, Ar), 4.38 (t, J = 6.9 Hz, 2H), 3.38 (t, J = 6.4 Hz, 2H), 2.07 (m, 2H), 1.92 (m, -CH$_2$-). 13C NMR (75 MHz, CDCl$_3$): δ 140.2, 125.7, 122.9, 120.4, 118.9, 108.5 (Ar), 42.1, 33.1, 30.2, 27.6 (-CH$_2$-). Anal. Calcd for C16H16BrN: C, 63.59; H, 5.34; N, 4.63. Found: C, 63.38; H, 5.25; N, 4.43%.

[16] F. Kröhnke, Synthesis 1 (1976) 1–24.

[17] J.P. Sadighi, R.A. Singer, S.L. Buchwald, J. Am. Chem. Soc. 120 (1998) 213–214.

[18] Synthesis of Ligand HL (3): 4-(p-Bromophenyl)-6-phenyl-2, 2′-bipyridine (1.94 g, 5.0 mmol), palladium acetate (13.0 mg, 0.06 mmol) and DPEphos (45.0 mg, 0.08 mmol) were charged into a flask and purged with argon. Aniline (1.0 mL, 10.7 mmol) was added via syringe, followed by toluene (20 ml). NaOBu^t (0.81 g, 8.5 mmol) was added in one portion. The reaction mixture was heated to 80 °C under stirring for 12 h. The solvent was removed by rotary evaporation. The residue was dissolved in dichloromethane, washed with distilled water, and dried over anhydrous sodium sulfate and concentrated. The residue was dissolved in THF (60 mL). NaH (2.5 g, >52%, in mineral oil) was added and purged with argon. The reaction mixture was stirred for 1 h at room temperature, and then 9-(4-bromobutane)carbazole (6.04 g, 20.0 mmol) was added dropwise via syringe. After the solution was refluxed until the conversion was complete (as monitored by thin layer chromatography), it was cooled to room temperature and poured into ice–water mixture slowly, extracted with CH$_2$Cl$_2$ until the water phase was colorless. The combined organic solutions were washed with distilled water, dried over anhydrous sodium sulfate and concentrated. The crude product was purified by column chromatography (silica gel, petroleum ether : CH$_2$Cl$_2$ = 2:1 (V/V) containing 5% (V) triethylamine). Ligand HL was obtained as pale yellow crystal by recrystallizing from MeOH/Ethyl Acetate solution: 1.7 g (yield: 54.8%). 1H NMR (300 MHz, CDCl$_3$): δ 8.74–8.66 (m, 3H), 8.20 (d, J = 7.2 Hz, 2H), 8.10 (d, J = 7.8 Hz, 2H), 7.95 (s, 1H), 7.90 (t, J = 7.5 Hz, 1H), 7.69 (d, J = 8.7 Hz, 2H), 7.55–7.43 (m, 5H), 7.38–7.30 (m, 5H), 7.23 (t, J = 6.9 Hz, 2H), 7.12–7.06 (m, 3H), 6.90 (d, J = 8.7 Hz, 2H, Ar), 4.33 (t, J = 7.0 Hz, 2H), 3.75 (t, J = 7.3 Hz, 2H), 2.04–1.94 (m, 2H), 1.86–1.76 (m, 2H,-CH$_2$-). Anal. Calcd for C44H36N4: C, 85.13; H, 5.85; N, 9.03. Found: C, 84.92; H, 5.67; N, 8.62%.

[19] Synthesis of Pt(II) complex (4): A mixture of HL (0.32 g, 0.5 mmol), K$_2$PtCl$_4$ (0.21 g, 0.5 mmol) and glacial acetic acid (30 mL) was refluxed for 24 h under a nitrogen atmosphere in the absence of light. The reaction mixture was then cooled to room temperature and filtered. The obtained solid was recrystallized from MeOH/CH$_2$Cl$_2$ solution twice to form the desired product as red crystal: 0.35 g (yield: 82.4%). 1H NMR (300 MHz, CDCl$_3$): δ 8.89 (d, J = 5.1 Hz, 1H), 8.68 (d, J = 8.1 Hz, 1H), 8.38 (s, 1H), 8.34 (t, J = 7.8 Hz, 1H), 8.14 (d, J = 7.8 Hz, 2H), 8.12 (d, J = 5.4 Hz, 1H), 7.92 (d, J = 8.7 Hz, 2H), 7.88 (t, J = 6.6 Hz, 1H), 7.75 (d, J = 7.5 Hz, 1H), 7.59 (d, J = 8.1 Hz, 1H), 7.50–7.36 (m, 5H), 7.21–7.04 (m, 8H),

6.85 (*d*, $J = 8.7$ Hz, 2H, Ar), 4.42 (*t*, $J = 6.9$ Hz, 2H), 3.80 (*t*, $J = 6.9$ Hz, 2H), 1.88 (*m*, 2H), 1.72 (*m*, 2H,-CH_2-). Anal. Calcd for C44H35ClN4Pt: C, 62.15; H, 4.15; N, 6.59. Found: C, 61.67; H, 4.11; N, 6.28%.

[20] Diffraction data was collected on a Bruker SMART APEX II CCD diffractometer equipped with a graphite-monochromated Mo-Kα radiation ($\lambda = 0.71073$ Å) at 296(2) K using a Φ–ω scan mode in the range of $2.38 \leq \theta \leq 25.00°$. A total of 17497 reflections including 6130 unique ones were collected, of which 6101 were observed [$I > 2\sigma$ (I)] and used in structure solution. The intensity data were corrected by Lp factors and empirical absorption The structure was solved by direct methods and subsequent successive difference Fourier maps, and refined by full-matrix least-squares techniques on F^2. All of the non-hydrogen atoms were refined anisotropically. The organic hydrogen atoms were generated geometrically.

[21] S.-W. Lai, M.C.-W. Chan, K.-K. Cheung, C.-M. Che, Organometallics 18 (1999) 3327–3336.

[22] J.H.K. Yip, Suwarno, J.J. Vittal, Inorg. Chem. 39 (2000) 3537–3543.

[23] S.-W. Lai, H.-W. Lam, W. Lu, K.-K. Cheung, C.-M. Che, Organometallics 21 (2002) 226–234.

[24] A. Hofmann, L. Dahlenburg, R. van Eldik, Inorg. Chem. 42 (2003) 6528–6538.

[25] G.M. Sheldrick, SHELXL 97, Program for Crystal Structure Refinement, University of Göttingen, Göttingen, Germany, 1997.

[26] G.M. Sheldrick, SHELXL 97, Program for Crystal Structure Solution, University of Göttingen, Göttingen, Germany, 1997.